약학석사학위논문

15-Keto Prostaglandin E_2 Inhibits Proliferation of Breast Cancer Cells through Suppression of STAT3 Signaling

STAT3 억제를 통한 15-Keto prostaglandin E_2의 인체 유방암세포 증식 억제 연구

2017년 2월

서울대학교 대학원

분자의학 및 바이오제약학과

이 은 지

Abstract

15-Keto Prostaglandin E_2 Inhibits Proliferation of Breast Cancer Cells through Suppression of STAT3 Signaling

Eun Ji Lee

Under the supervision of Professor Young-Joon Surh

Department of Molecular Medicine and Biopharmaceutical Science

Seoul National University

Prostaglandin E_2 (PGE_2) is highly produced during inflammation and cancer. Overproduction of PGE_2 has been associated with increased tumor cell proliferation, resistance to apoptosis and invasiveness. PGE_2 is oxidized to 15-keto prostaglandin E_2 (15-keto PGE_2) by 15-hydroxyprostaglandin dehydrogenase (15-PGDH). 15-Keto PGE_2 is considered as a biologically inactive form of the pro-tumorigenic lipid mediator, PGE_2. However, recent studies have revealed that 15-keto PGE_2 has tumor suppressive functions, but the underlying molecular mechanisms remain to be elucidated. Signal transducer and activator of transcription 3 (STAT3) is a transcription factor that regulates transcription of genes involved in cell proliferation, cell cycle progression and cell survival. It is constitutively activated in most of cancer types, and the aberrantly activated STAT3 contributes to tumor promotion and progression. This prompted me to investigate the effects of 15-keto PGE_2 on STAT3 activation. Notably, 15-keto PGE_2 containing an α,β-unsaturated carbonyl group directly bound to STAT3 and thereby

suppressed the phosphorylation, dimerization and nuclear translocation of this transcription factor in Ha-*Ras* transformed human mammary epithelial (MCF10A-*ras*) cells. In contrast, its non-electrophilic analogue, 13,14-dihydro-15-keto PGE_2 failed to inhibit the STAT3 activation and was unable to suppress the growth and transformation of MCF10A-*ras* cells. Moreover, thiol reducing agents, such as dithiothreitol or N-acetyl-L-cysteine, disrupted the interaction between 15-keto PGE_2 and STAT3, and abrogated STAT3 inactivation by 15-keto PGE_2. A molecular docking analysis suggests that Cys^{251} and Cys^{259} residues of STAT3 are preferential binding sites for this lipid mediator. In addition, subcutaneous injection of 15-keto PGE_2 attenuated xenograft tumor growth and decreased phosphorylated STAT3 in athymic nude mice transplanted with human breast cancer MDA-MB-231 cells. Taken together, thiol modification of STAT3 by 15-keto PGE_2 inhibits STAT3 activation, thereby suppressing breast cancer cell proliferation, growth and transformation.

Keywords: 15-Keto PGE_2, electrophile, α,β-unsaturated carbonyl group, STAT3, thiol modification, MCF10A-*ras*, MDA-MB-231 xenografts

Student Number: 2015-26014

Contents

List of Figures

Introduction

Prostaglandin E_2 (PGE_2) is an inflammatory lipid mediator produced as one of the major products of the arachidonic acid metabolism catalyzed by cyclooxygenase-2 (COX-2) during inflammation [1]. Production of PGE_2 increases upon inflammatory insults, and its levels are abnormally elevated in various human malignancies [2, 3] including breast cancer [4]. There is a close association between inflammation and cancer [5]. COX-2-derived PGE_2 has been known to play a key role in inflammation-associated cancer progression [6].

PGE_2 exerts its function by binding to specific cell surface receptors, called EP receptors [7, 8]. PGE_2-induced overactivation of EP receptors can accelerate cancer progression through modulation of several intracellular signaling pathways [9-11]. Signal transducer and activator of transcription 3 (STAT3) is a transcription factor that regulates cellular processes involved in proliferation, development, inflammation and cell survival [12]. In response to extracellular stimuli, such as cytokines and growth factors, STAT3 is recruited from the cytosol to their receptors and is phosphorylated by receptor-associated janus kinase (JAKs) [13]. Phosphorylation of the tyrosine 705 residue of STAT3 induces a dimer formation and, then the resulting dimer complex translocates to the nucleus for initiating transcription of target genes [14]. Aberrant activation of STAT3 is linked to tumorigenesis [15]. In contrast to the transient STAT3 activation in normal cells, most of cancer cells retain constitutively activated STAT3 activity [16]. For instance, STAT3 is overactivated in more than 40% of breast cancers [17]. Therefore, targeting abnormally overactivated STAT3 signal transduction has been suggested as a therapeutic strategy in the management of cancer [16, 18, 19]. Many

studies revealed a positive correlation between PGE_2 overproduction and STAT3 overactivation in prostate, lung, bladder and colorectal cancers [20-22]. Therefore, it is likely that the PGE_2-STAT3 axis has a crucial role in tumorigenesis.

PGE_2 undergoes oxidation by 15-hydroxyprostaglandin dehydrogenase (15-PGDH) to produce 15-keto PGE_2 which has been considered biologically inactive [23]. However, recent studies have revealed that 15-keto PGE_2 has antitumor functions. Thus, 15-keto PGE_2 has been reported to induce apoptosis of pancreatic adenocarcinoma through production of ROS [24]. The 15-keto PGE_2-induced oxidative stress was attributable to its suppression of expression of *xCT* and *CTH* encoding, respectively a light-chain subunit of cystine-glutamate exchange transporter and cystathionine γ-lyase that play key roles in providing cellular cysteine supply for glutathione biosynthesis. The cell death-promoting effect of 15-keto-PGE_2 is mediated partly but not entirely through PPARγ activation [24]. In another study, 15-keto PGE_2 was demonstrated to inhibit hepatocellular carcinoma growth through PPARγ-mediated activation of $p21^{WAF/Cip1}$ [25]. Thus, the mechanisms underlying cytotoxic effects of 15-keto PGE_2 appear to be different, depending on the cancer cell type.

15-Keto PGE_2 has an α,β-unsaturated carbonyl moiety [26], and hence can act as a Michael addition acceptor. The electrophilic α,β-unsaturated carbonyl group modifies the nucleophilic thiol group of cysteine residue(s) in various proteins [27-29]. For instance, 15-keto PGE_2 can act as a PPARγ ligand through the Michael addition to the cysteine residue of this transcription factor [26, 30]. Similarly, cysteine residues contained in STAT3 are speculated targets of 15-keto PGE_2. In this study, I investigated whether 15-keto PGE_2 could bind and subsequently inactivate STAT3, thereby suppressing human breast cancer cell proliferation and growth. I found that the

electrophilic α,β-unsaturated carbonyl group of 15-keto PGE_2 covalently modifies STAT3 thiol residue(s) and prevents STAT3 activation.

Materials and Methods

Cell culture

MCF10A and MCF10A-*ras* cells were cultured in Dulbecco's Modified Eagle Medium: Nutrient Mixture-F-12 (DMEM/F-12) supplemented with 5% heat-inactivated horse serum from Gibco (Grand Island, NY, USA), 10 μg/ml insulin, 100 ng/ml cholera toxin, 0.5 μg/ml hydrocortisone, 20 ng/ml human epidermal growth factor, 2 mmol/L L-glutamine and 100 units/ml penicillin/streptomycin. MDA-MB-231 and HeLa/P-STAT3-Luc cells were maintained in DMEM supplemented with 10% fetal bovine serum (FBS) from GenDEPOT (Barker, TX, USA) and 1% antibiotic-antimycotic mixture. PC3 cells were cultivated in RPMI 1640 containing 10% heat-inactivated FBS from GenDEPOT and 1% antibiotic-antimycotic mixture. These cell lines were grown at 37°C in humidified atmosphere of 5% CO_2.

Chemicals

15-Keto PGE_2 (9,15-dioxo-11α-hydroxy-prosta-5Z,13E-dien-1-oic acid) and 13-14-dihydro-15-keto PGE_2 (9,15-dioxo-11α-hydroxy-prosta-5Z-en-1-oic acid) were purchased from Cayman Chemicals (Ann Arbor, MI, USA). Dithiothreitol (DTT) and N-acetyl-L-cysteine (NAC) were purchased from Sigma Chemical Co. (St. Louis, MO, USA). Primary antibodies for STAT3, P-STAT3^{Y705}, JAK2 and P-JAK2 were supplied from Cell Signaling Technology (Danvers, MA, USA). Actin and lamin B antibodies were supplied from Santa Cruz Biotechnology (Santa Cruz, CA, USA). 15-PGDH primary antibody was obtained from Cayman Chemicals. Anti-rabbit and anti-mouse horseradish peroxidase conjugated secondary antibodies were purchased from Zymed

Laboratories Inc. (San Francisco, CA, USA).

Western Blot Analysis

Preparation of cell lysates

After treatment with 15-keto PGE_2 or 13,14-dihydro-15-keto PGE_2, MCF10A-*ras* cells were harvested at indicated time points. The cells were rinsed with cold phosphate-buffered saline (PBS) and then scraped in 1 ml PBS followed by centrifugation at 1,700 *g* for 5 min at 4℃. Whole cell lysates were prepared with 10x Cell Lysis Buffer purchased from Cell Signaling Technology diluted to 1x solution containing 1% of phenylmethylsulfonyl fluoride (PMSF). Cell pellets were resuspended and incubated for 1 h on ice followed by centrifugation at 18,000 *g* for 15 min. Supernatant was collected as whole cell lysates. For obtaining cytosolic and nuclear extracts, buffer A was used for cytosolic extracts and buffer C for nuclear extracts. Pellets were resuspended in hypotonic buffer A [10mM HEPES (pH 7.9), 1.5 mM $MgCl_2$, 10 mM KCl, 0.5 mM DTT and 0.2 mM PMSF] for 15 min on ice, and 0.1% nonidet P-40 (NP-40) was added for less than 5 min. The mixture was then centrifuged at 6,000 *g* for 5min at 4℃. The supernatant contained cytosolic protein. The pellets were rinsed twice with hypotonic buffer A and resuspended again in hypertonic buffer C [20 mM HEPES (pH 7.9), 1.5 mM $MgCl_2$, 420 mM NaCl, 0.5 mM DTT, 0.2 mM PMSF, 0.2 mM EDTA and 20% glycerol]. After incubation for 1 h on ice, the mixtures were centrifuged at 18,000 *g* for 15 min at 4℃. Supernatant was collected as nuclear extract.

Quantification of the protein concentration

Protein concentrations in whole cell lysates were determined by using the BCA

protein assay kit supplied from ThermoFisher Sientific (Rockford, IL, USA). Protein concentrations in cytosolic and nuclear extracts were determined by using the Bradford Assay Reagents kit purchased from Bio-Rad (Hercules, CA, USA).

Sodium Dodecyl Sulphate-Polyacrylamide Gel Electrophoresis (SDS-PAGE)

Equivalent amounts of protein from whole cell lysate or nuclear fraction were mixed with SDS sample loading dye and boiled for 5 min at 99℃. Protein samples were resolved by SDS-PAGE and transferred to polyvinylidene fluoride (PVDF) microporous membrane supplied from PALL Corporation (Port Washington, NY, USA). Non-specific antibody binding sites were blocked by 3% skim milk in PBS containing 0.05% Tween 20 (PBST) for 1 h at room temperature. Membranes were washed and followed by incubation in PBST containing specific primary antibodies for each condition. The membranes were rinsed three times again and incubated with respective horseradish peroxidase conjugated secondary antibodies for 1 h at room temperature. Peroxidase activity was detected by incubating in ECL reagent for 5 min according to the manufacturer's instruction and visualized using the imagequant LAS-4000 purchased from Fujifilm Life Science (Stamford, CT, USA)

Reverse transcription-polymerase chain reaction (RT-PCR)

Total RNA was isolated from MCF10A-*ras* cells by using TRIzol® supplied from Invitrogen (Carlsbad, CA, USA) according to the manufacturer's protocol. To generate cDNA, 1 μg of total RNA was reverse transcribed with murine leukemia virus reverse transcriptase purchased from Promega (Madison, WI, USA) for 50 min at 42℃ and again for 15 min at 72℃. The cDNA sample (1 μl) was amplified in sequential reactions.

The mRNA expression of GAPDH and STAT3 target genes (*MCP-1*, *CCL-5*, *Cyclin D1*, *p21* and *Bcl-xL*) was determined according to following conditions.

Gene name	Sequence		Cycles	Tm
GAPDH	Forward	5'-GCA TGG CCT TCC GTG TCC CC-3'	28	62
	Reverse	5'-CAA TGC TGG CCC CAG CGT CA-3'		
MCP-1	Forward	5'-TGC TCA TAG CAG CCA CCT TC-3'	33	55
	Reverse	5'-GTC CAT GGA ATC CTG AAC CC-3'		
CCL-5	Forward	5'-CGT GCC CAC ATC AAG GAG-3'	33	52
	Reverse	5'-GGA CAA GAG CAA GCA GAA AC-3'		
Cyclin D1	Forward	5'-ACC TGG ATG CTG GAG GTC T-3'	28	57
	Reverse	5'-GCT CCA TTT GCA GCA GCT C-3'		
p21	Forward	5'-AAT CTG TCA TGC TGG TCT GC-3'	25	58
	Reverse	5'-ACT GTG ATG CGC TAA TGG C-3'		
Bcl-xL	Forward	5'-GGA AAG CGT AGA CAA GGA-3'	25	62
	Reverse	5'-GGT GGG AGG GTA GAG TGG-3'		

Amplification products were resolved by 3% agarose gel electrophoresis, stained with SYBR green and photographed using fluorescence in LAS-4000.

STAT3 promoter luciferase reporter gene assay

HeLa cells were transfected with P-STAT3-TA-luc vector supplied from Clontech (Mountain View, CA, USA) with FuGENE from Promega according to supplier's instructions. The HeLa/P-STAT3-Luc cells were seeded at a density of 8 x 10^4 per well in six-well plates. Cells were pretreated with 15-keto PGE_2 or 13,14-dihydro-15-keto

PGE_2 for 24 h and then stimulated with 10 ng/ml of Oncostatin M for 6 h. The cells were washed by PBS and lysed in 1x reporter lysis buffer from Promega. Twenty μl of lysed cell extract were mixed with 100 μl of the luciferase substrate, and the luciferase activity was determined using a luminometer (AutoLumat LB 953, EG&G Berthold). The β-galactosidase activity was measured to normalize the luciferase activity.

Wound migration assay

The Culture-Insets (Ibidi) were transferred to 6-well plates. MCF10A and MCF10A-*ras* cells were seeded at a density of 5 x 10^4 cells per well in Culture-Inserts. After 24 h, the silicon inserts were removed, and the cells were photographed under a microscope. The separated walls were closed after 24 h, and these closed gap images were captured using a microscope.

Clonogenic assay

MCF10A-*ras* cells were plated in 6-well plates at a density of 200 cells per well. The DMEM/F-12 medium was changed every another day and treated with 15-keto PGE_2 (20 μM) or 13,14-dihydro-15-keto PGE_2 (20 μM). After 7 days, the cells formed colonies. The colonies were fixed in cold methanol and stained by 0.5% crystal violet. The stained colonies were washed with PBS to remove excessive dye. Quantitative changes in clonogenicity were determined by extracting stained dye with 10% acetic acid and measured the absorbance of the extracted dye at 570 nm.

Anchorage independent growth assay

MCF10A-*ras* cells were plated on a 60 mm dish containing 0.5% (down) and 0.33%

(up) double layer agar. The dishes were incubated at 37℃ in humidified incubator for 21 days. The cells were treated day after day with DMEM/F-12 containing DMSO, 15-keto PGE_2 (20 μM) or 13,14-dihydro-15-keto PGE_2 (20 μM). The colonies were stained with crystal violet for 12 h and rinsed with PBS. The number of colonies was counted by the ECLIPSE Ti inverted microscope and the NIS-Elements AR (V.4.0) computer software program (NIKON Instruments Korea, Seoul, Korea).

Immunoprecipitation

MCF10A-*ras* cells were plated in a 100 mm dish and treated with 15-keto PGE_2 (20 μM), 13,14-dihdro-15-keto PGE_2 (20 μM) or biotinylated 15-keto PGE_2 (40 μM) for indicated time. The cells were washed with ice-cold PBS and lysed in 1x lysis buffer for 1 h on ice followed by centrifugation at 18,000 *g* for 15 min. The protein concentration was determined by using the BCA protein assay kit (Pierce, Rockford, IL, USA). Cell lysates (500 μg) were subjected to immunoprecipitation by shaking with primary STAT3 antibody and protein A/G agarose bead suspension at 4℃ for 12 h. After centrifugation at 18,000 *g* for 1 min, immunoprecipitation beads were collected by pouring the supernatant and washed with cell lysis buffer. The immunoprecipitation beads were then mixed with 25 μl of 2x SDS electrophoresis sample buffer and boiled for 5 min at 99℃. Supernatant (25 μl) from each sample was collected by centrifugation and loaded on SDS-polyacrylamide gel. For exogenous STAT3 homo-dimerization, PC3 cells were co-transfected with HA-tagged and Myc-tagged constitutively active STAT3s. The transfected PC3 cells were treated with 15-keto PGE_2 (20 μM) or 13,14-dihydro-15-keto PGE_2 (20 μM) for 12 h. Lysates from transfected PC3 cells were immunoprecipitated

with indicated antibodies.

Immunocytochemistry

MCF10A-*ras* cells were plated on the 8-well chamber slides at a density of 1 x 10^4 per well and treated with 15-keto PGE_2 or 13,14-dihydro-15-keto PGE_2. Cells were fixed in 4% formaldehyde for 15 min at 37℃. After rinse with PBST, cells were treated with 0.1% Triton X-100 in PBS for 5 min and washed with PBST. Samples were blocked with 0.05% Tween-20 in PBS containing 5% bovine serum albumin (BSA) at room temperature for 30 min and washed with PBST and then incubated with diluted (1:200) primary antibody for overnight at 4℃. After washing with PBST, samples were incubated with a diluted (1:1000) TRITC-conjugated anti-mouse secondary antibody in PBST containing 5% BSA at room temperature for 1 h. Samples were washed with 0.05% PBST containing 5% BSA then examined under a fluorescent microscope.

Docking study

A docking study was performed using covalent docking modules implemented in Maestro v9.5 (Schrödinger LLC, NY). The STAT3 crystal structure (PDB code: 1BG1) was retrieved from PDB bank. The protein structure and ligand were prepared according to the standard procedure of the Protein Preparation Wizard and Ligprep modules in Maestro v9.5. After adding hydrogens, STAT3 protein was neutralized and then energically minimized on only hydrogens. The structure of 15-keto PGE_2 was drawn by ionization at pH 7.4 and energy minimization. 15-Keto PGE_2 was docked to the molecular model of STAT3 *in silico*. In covalent docking module, the reaction type was set to Micheal addition between Cys^{251} or Cys^{259} of STAT3 protein and C13 atom of 15-

keto PGE_2. The grid box was automatically determined the residues within 5.0 Å of the Cys^{251} or Cys^{259} residue in STAT3. After minimization of residues within 3 Å of covalently bound ligand, the outputs 10 poses of ligand-receptor complex was scoring by Prime MM-GBSA to calculate a binding affinity. The best binding energy of 15-keto PGE_2, low PrimeΔG_{bind}, was chosen for the binding mode analysis.

Xenograft model

BALB/c (nu/nu) athymic mice were purchased from Charles River Laboratories (Skokie, IL, USA) and kept in a room at constant temperature (24 ± 2℃) and humidity (50 ± 10%). The animal study was approved by Seoul National University Institutional Animal Care and Use Committees (IACUC). Seven-week old female BALB/c nude mice were subcutaneously injected with 2 x 10^6 MDA-MB-231 cells per mouse at both flanks. After 10 days, mice were randomly assigned to three groups (seven mice per group) and were treated with vehicle (5% DMSO in PBS), 15-keto PGE_2 (70 μg/kg) or 15-keto PGE_2 (140 μg/kg) daily by s.c. injection for 4 weeks. Tumor volumes were measured every other day with a digital caliper and calculated by the formula 0.52 x length x $width^2$. Mice were weighed three times a week.

Hematoxylin and eosin (H&E) staining and immunohistochemical analysis (IHC) of xenograft tumors

The MDA-MB-231 xenograft tumors were removed and fixed in formalin solution (10% neutral buffered formaldehyde) at room temperature for 48 h. Slides containing 4 μm section of formalin-fixed and paraffin-embedded specimens of xenograft tumors were prepared for histopathological and immunohistochemical analyses. H&E staining

was carried out as described previously [31]. The tumor sections were used to determine the expression of P-STAT3^{Y705} by immunohistochemical analysis. Slide incubated with primary antibodies for P-STAT3^{Y705} and developed using anti-rabbit horseradish peroxidase Envision System (DAKO). The counterstaining was done using Mayer's hematoxylin.

Statistical analysis

Statistical analysis for single comparison was performed using the Student's *t*-test. Data were expressed as means of ± SD at least three independent experiments. $p < 0.05$ was considered a statistically significant difference.

Results

The relationship between cellular PGE_2 levels and STAT3 phosphorylation in MCF10A-ras cells compared to non-oncogenic MCF10A

Arachidonic acid generates PGE_2 through the action of COX-2. 15-PGDH oxidizes the 15(S)-hydroxyl group of PGE_2 to generate 15-keto PGE_2 **(Fig. 1A)** [23, 32]. The PGE_2-STAT3 axis plays a key role in cancer cell growth and metastasis in several cancer types [20-22, 33]. In human breast cancer cells, PGE_2 production was elevated compared to normal cells [34].

Total lysates of MCF10A and MCF10A-*ras* cells were analyzed for the basal levels of COX-2, 15-PGDH, STAT3 and phosphorylated STAT3. The protein level of 15-PGDH was higher in normal breast MCF10A cells compared to oncogenic MCF10A-*ras* cells. However, the levels of COX-2 and phosphorylated STAT3 were significantly elevated in MCF10A-*ras* cells **(Fig. 1B)**. The result showed a positive correlation between COX-2 and phosphorylated STAT3 whereas there was an inverse relationship between 15-PGDH and COX-2 or P-$STAT3^{Y705}$. Moreover, the wound healing ability in MCF10A-*ras* cells is greater than that in non-oncogenic MCF10A cells **(Fig. 1C)**.

Inhibitory effects of 15-Keto PGE_2 on STAT3 phosphorylation in MCF10A-ras cells

Phosphorylation of STAT3 at tyrosine 705 is known to be an important event for activation of this transcription factor and is implicated in cancer progression [35]. 15-Keto PGE_2 significantly decreased STAT3 phosphorylation in a dose- **(Fig. 2A)** and time-dependent manner **(Fig. 2B)**.

PPARγ has been known to be an anticancer target [36]. Recent studies show that the oxidized prostaglandin metabolites modulate PPARγ activity as endogenous ligands of

this transcription factor [30]. 15-Keto PGE_2 is one of oxidized forms of prostaglandins and exerts antitumor effects by activating PPARγ [25, 26]. However, suppression of STAT3 phosphorylation through 15-keto PGE_2 did not appear to depend on PPARγ activity as nuclear accumulation of this transcription factor was not much different between control and 15-keto PGE_2-treated groups **(Fig. 2C)**. Next, I investigated whether 15-keto PGE_2 could inhibit STAT3 phosphorylation through regulation of JAK2, a well-known kinase responsible for STAT3 phosphorylation [35, 37, 38], and suppressor of cytokine signaling 3 (SOCS3), a STAT3 negative regulator [39]. 15-Keto PGE_2 (20 μM) affected neither JAK2 phosphorylation nor SOCS3 expression while STAT3 phosphorylation was suppressed (**Fig. 2D**).

Inhibition of STAT3 dimerization and nuclear translocation by 15-Keto PGE_2

Phosphorylated STAT3 forms a homodimer, accumulates in the nucleus, binds to specific DNA sequences and then initiates transcription of target genes [40]. Treatment of MCF10A-*ras* cells with 10 or 20 μM of 15-keto PGE_2 resulted in interference of STAT3 homodimerization **(Fig. 3A)**. As a consequence, P-$STAT3^{Y705}$ barely accumulated in the nucleus of 15-keto PGE_2-treated cells **(Fig. 3B and C)**.

15-Keto PGE_2-mediated inhibition of MCF10A-ras cell proliferation and growth through suppression of transcription of STAT3 target genes

Dimerized STAT3 localizes in the nucleus [14], where it regulates the expression of target genes. To assess the effect of 15-keto PGE_2 on transcriptional activity of STAT3, I performed a luciferase reporter gene assay. 15-Keto PGE_2 inhibited the Oncostatin M

(OSM)-induced STAT3 transcriptional activity in HeLa/P-STAT3-Luc cells **(Fig. 4A)**.

Nuclear translocated STAT3 binds to the promoters of numerous target genes [41]. Some of the protein products of STAT3 target genes have oncogenic functions [42]. These include monocyte chemoattractant protein-1 (MCP-1), chemokine (C-C motif) ligand 5 (CCL5), cyclin D1, Bcl-xL, $p21^{WAF/Cip1}$ (cyclin-dependent kinase inhibitor 1) and myeloid cell leukemia 1 (MCL-1). 15-Keto PGE_2 modulated the expression of these STAT3 target genes **(Fig. 4B)**. The clonogenic assay and the anchorage-independent growth assay were conducted to investigate anti-proliferative effects of 15-keto PGE_2. Results show that 15-keto PGE_2 treatment markedly reduced the colony formation **(Fig. 4C and D).**

The involvement of the α,β-unsaturated carbonyl moiety of 15-Keto PGE_2 in STAT3 deactivation

15-Keto PGE_2 has an α,β-unsaturated carbon which is capable of interacting with nucleophilic cellular proteins [26]. In contrast to 15-keto PGE_2, 13,14-dihydro-15-keto PGE_2 that lacks an electrophilic α,β-unsaturated carbonyl group **(Fig. 5A)** failed to inhibit STAT3 phosphorylation **(Fig. 5B)**. In addition, 13,14-dihydro-15-keto PGE_2-treated MCF10A-*ras* cells did not exhibit a significant change in homodimerization **(Fig. 5C)**. PC3 cells were transfected with HA-tagged STAT3 and Myc-tagged STAT3 followed by treatment with 15-keto PGE_2 (20 μM) or 13,14-dihydro-15-keto PGE_2 (20 μM), and the immunoprecipitation assay was conducted. The STAT3 dimerization was inhibited by 15-keto PGE_2 but not by 13,14-dihydro-15-keto PGE_2 **(Fig. 5D)**. Likewise, the nuclear accumulation of phosphorylated STAT3 was not attenuated by 13,14-dihydro-15-keto PGE_2 as well **(Fig. 5E and F)**. Furthermore, the transcriptional activity

of STAT3 was again not affected by 13,14-dihydro-15-keto PGE_2 **(Fig. 5G)**. The colony formation was suppressed by 15-keto PGE_2 but not by 13,14-dihydro-15-keto PGE_2 **(Fig. 5H and I)**. Above results suggest that the electrophilic α,β-unsaturated carbonyl group of 15-keto PGE_2 is important for deactivating STAT3.

Covalent binding of 15-Keto PGE_2 to STAT3 via Michael addition reaction

The electron-poor-β-carbon in the α,β-unsaturated carbonyl group attacks electron-rich nucleophiles, forming a covalent bond via Michael addition reaction [43, 44]. As shown in **Fig. 6A**, 15-keto PGE_2 harboring the electrophilic α,β-unsaturated carbonyl moiety is supposed to covalently bind to thiol group(s) of STAT3. To investigate a putative covalent interaction between 15-keto PGE_2 and a thiol group of STAT3, MCF10A-*ras* cells were pretreated with thiol reducing agents, such as DTT and NAC. The inhibition of STAT3 phosphorylation by 15-keto PGE_2 was abolished by DTT or NAC treatment **(Fig. 6B)**. To investigate direct interaction between 15-keto PGE_2 and STAT3, an immunoprecipitation assay using the biotin-streptavidin system was performed. The result showed that biotinylated 15-keto PGE_2 directly bound to STAT3 **(Fig. 6C)**. However, DTT and NAC abrogated the interaction between 15-keto PGE_2 and STAT3 **(Fig. 6D)**. A docking model predicted that Cys^{251} and Cys^{259} of STAT3 as putative binding sites of 15-keto PGE_2 **(Fig. 6E)**. Taken together, these data suggest that 15-keto PGE_2 covalently interacts with STAT3 through thiol modification of this transcription factor.

Suppression of tumor growth and STAT3 phosphorylation by 15-Keto PGE_2 in a MDA-MB-231 xenograft model

When human breast cancer MDA-MB-231 cells were treated with 10 or 20 μM of 15-keto PGE_2, colony formation was repressed **(Fig. 7A)**. The expression of phosphorylated STAT3 was significantly decreased by 15-keto PGE_2 in MDA-MB-231 cells **(Fig. 7B)**. I examined whether 15-keto PGE_2 has anti-tumor activity in MDA-MB-231 cells transplanted to BALB/c nude mice. The mice xenografted with MDB-MB-231 cells were subcutaneously injected with two different doses (70 μg/kg and 140 μg/kg) of 15-keto PGE_2 for 4 weeks. The tumor growth was significantly retarded in 15-keto PGE_2-injected mice groups **(Fig. 7C and D).** The average tumor volume in 15-keto PGE_2-treated mice was dramatically reduced in a dose-dependent manner **(Fig. 7E)**. Under these experimental conditions, there were no body weight loss and other signs of toxicity in mice treated with 15-keto PGE_2 **(Fig. 7F)**. Histopathological analysis of the tumor samples stained for H&E showed that tumor density was decreased in 15-keto PGE_2-treated mice compared to that in the control animals **(Fig. 7G)**. Furthermore, the phosphorylation of STAT3 was markedly decreased in the group treated with the higher dose (140 μg/kg) of 15-keto PGE_2 **(Fig. 7H)**. Immunohistochemical analysis of tumor samples showed that the expression of P-STAT3^{Y705} was significantly reduced in the group treated with the higher dose (140 μg/kg) of 15-keto PGE_2, supporting the western blotting data (**Fig. 7I**).

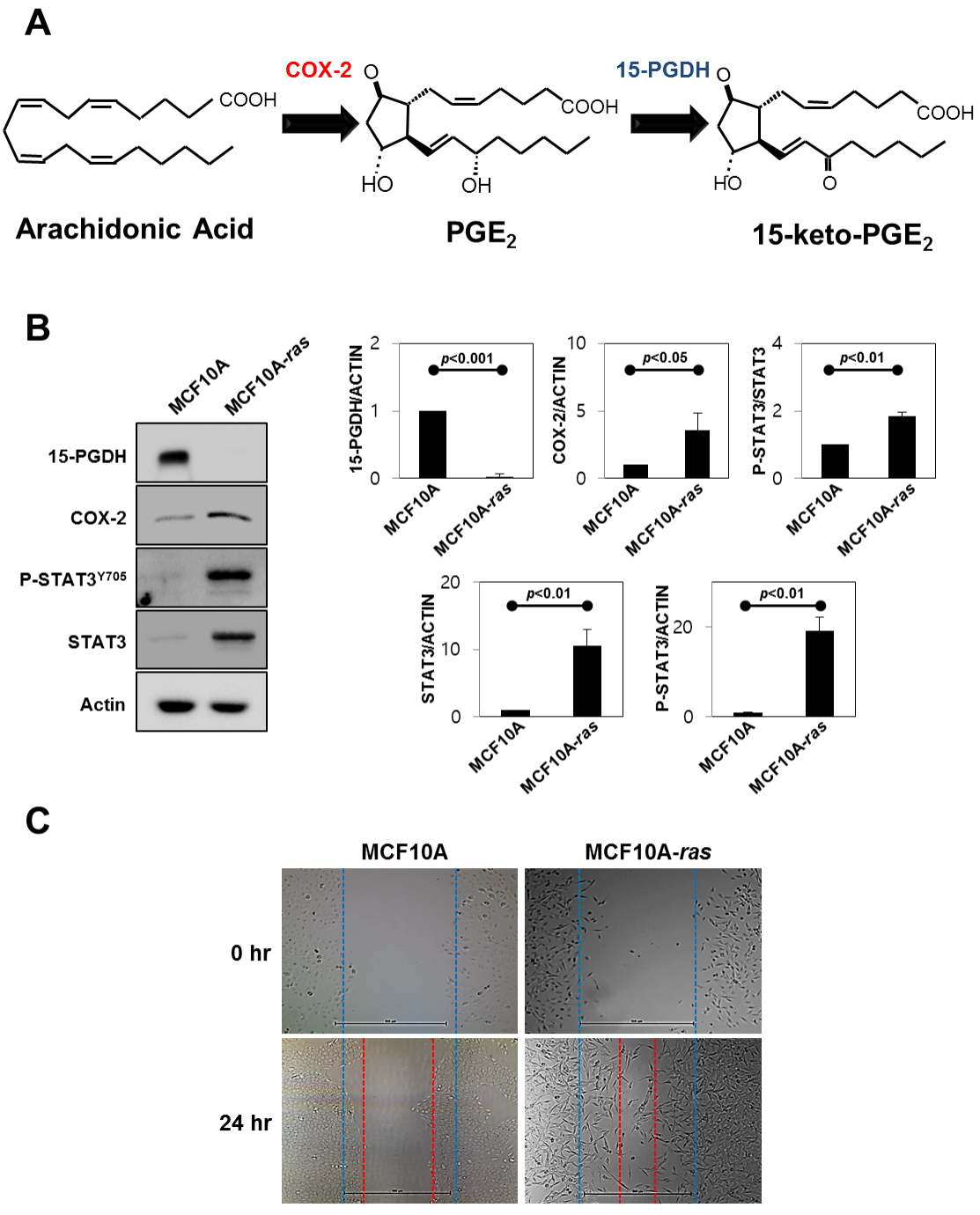

Figure 1. The relationship between cellular PGE_2 levels and STAT3 phosphorylation in MCF10A-*ras* cells compared to non-oncogenic MCF10A A. A scheme of PGE_2 synthesis and degradation. PGE_2 is synthesized by COX-2 and degraded by 15-PGDH. 15-Keto PGE_2 is an oxidized metabolite of PGE_2. **B.** The

protein levels of 15-PGDH, COX-2, STAT3 and P-STAT3^{Y705} were compared in non-oncogenic MCF10A and MCF10A-*ras* cells by Western blot analysis. Actin was used as a loading control. **C.** The migration of MCF10A and MCF10A-*ras* cells was assessed by measuring the width of un-migrated space under a microscope.

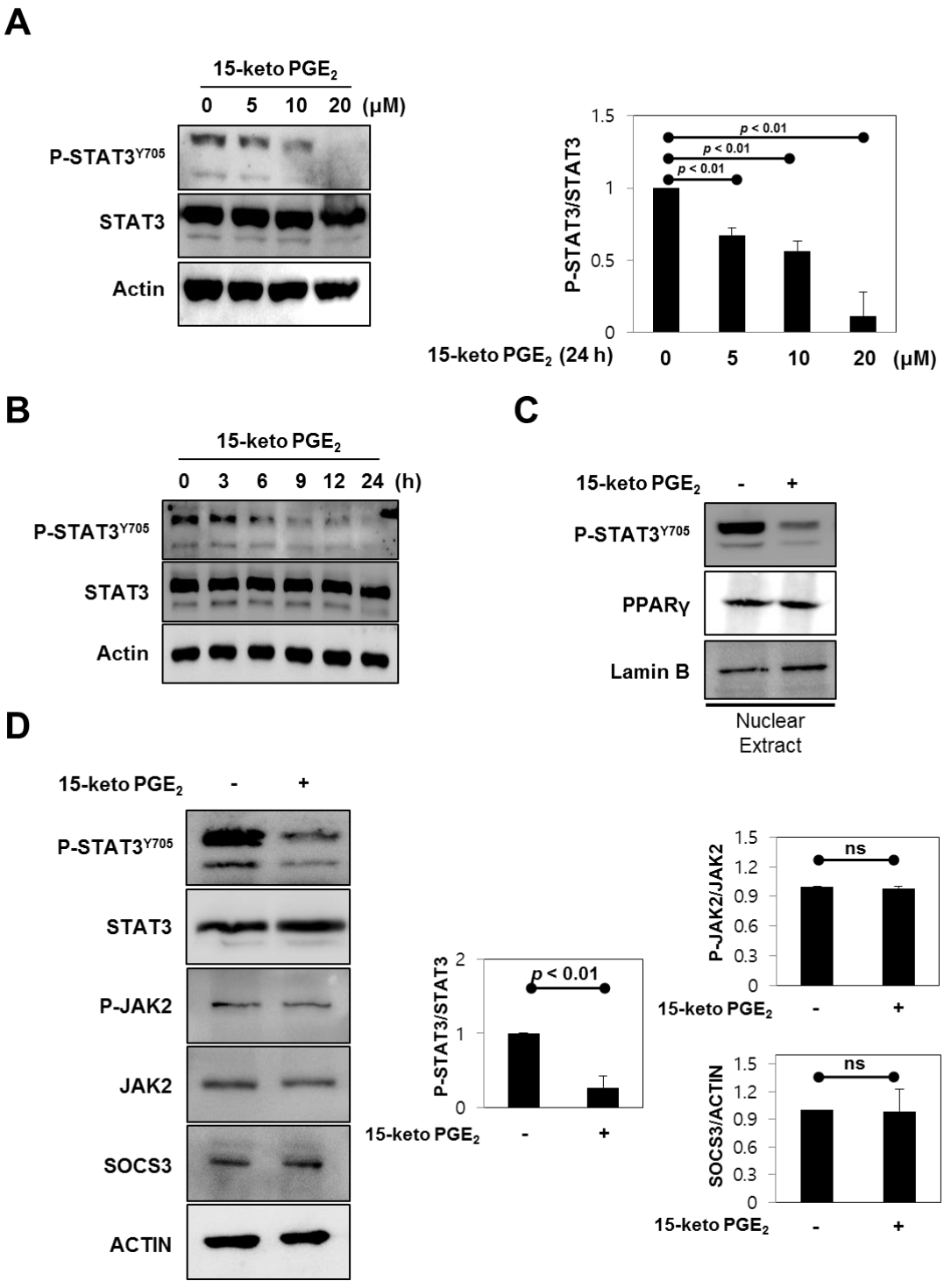

Figure 2. Inhibitory effects of 15-Keto PGE_2 on STAT3 phosphorylation in MCF10A-*ras* cells A. MCF10A-*ras* cells were treated with indicated concentrations of 15-keto PGE_2 for 24 h. The expression levels of STAT3 and P-$STAT3^{Y705}$ were

determined by Western blot analysis. **B.** MCF10A-*ras* cells were incubated with 15-keto PGE_2 (20 μM) for indicated time periods. The protein level of phosphorylated STAT3 was measured by Western blotting. **C.** Nuclear extracts were isolated from 15-keto PGE_2 (20 μM)-treated MCF10A-*ras* cells, and nuclear PPARγ levels were analyzed by Western blot analysis. **D.** MCF10A-*ras* cells were treated with 15-keto PGE_2 (20 μM) for 24 h. The expression of JAK2, an upstream kinase of STAT3 and SOCS3, a negative regulator of STAT3, were assessed by Western blot analysis.

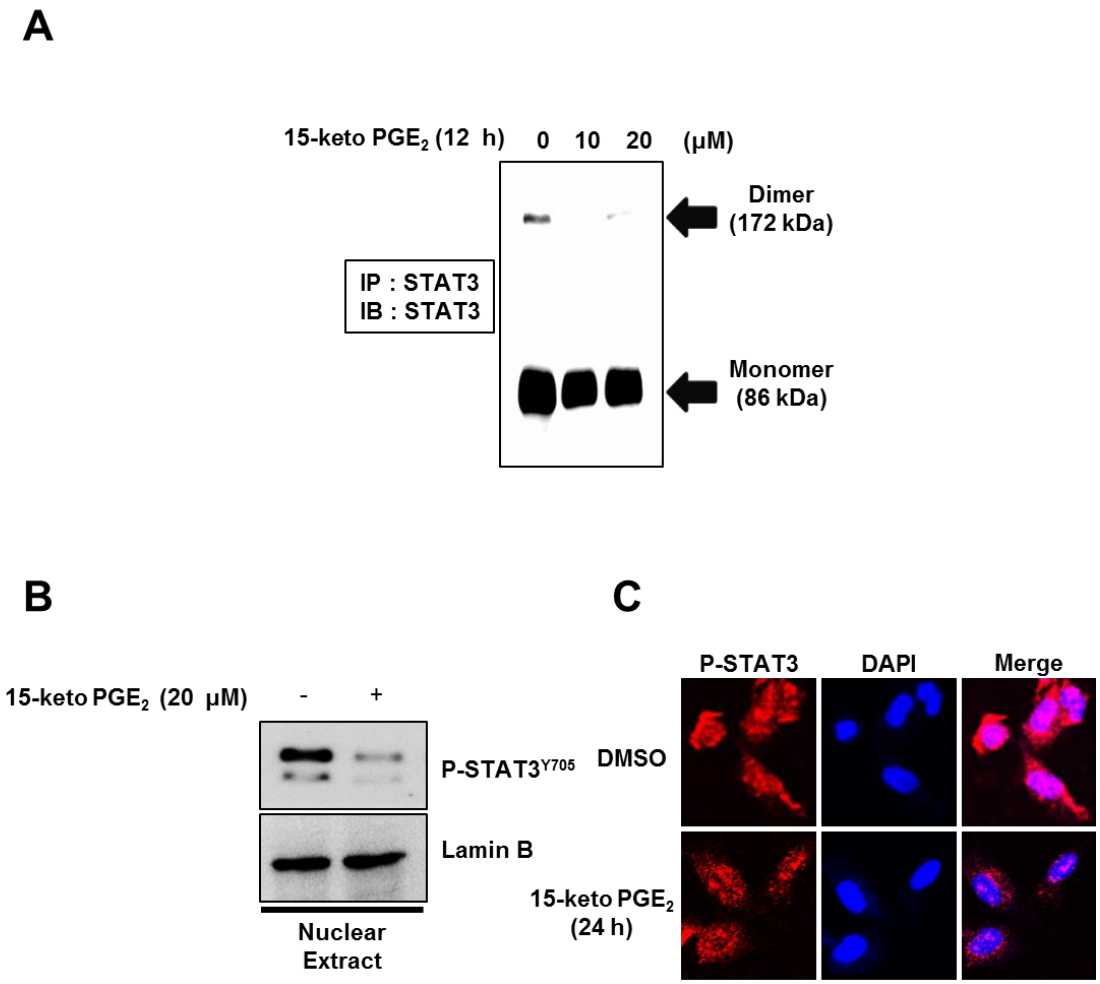

Figure 3. Inhibition of STAT3 dimerization and nuclear translocation by 15-Keto PGE_2 A. Whole lysates from MCF10A-*ras* cells treated with two different concentrations of 15-keto PGE_2 (10 or 20 μM) for 12 h were prepared for immunoprecipitation of STAT3 protein using protein A/G agarose conjugated C-terminus anti-STAT3 antibody. The STAT3 homodimerization was analyzed by Western blot analysis using N-terminus anti-STAT3 antibody. **B.** Nuclear extracts were immunoblotted for detecting P-$STAT3^{Y705}$ localization. MCF10A-*ras* cells were treated with 15-keto PGE_2 (20 μM). After 24 h, the cells were harvested. Lamin B was used as loading control in nuclear extract. **C.** Immunocytochemical analysis was performed

using antibodies against P-STAT3^{Y705}. MCF10A-*ras* cells were treated with or without 15-keto PGE_2 (20 μM) for 24 h. Nuclei were stained with DAPI and visualized under a confocal microscope. Two images were merged to verify co-localization.

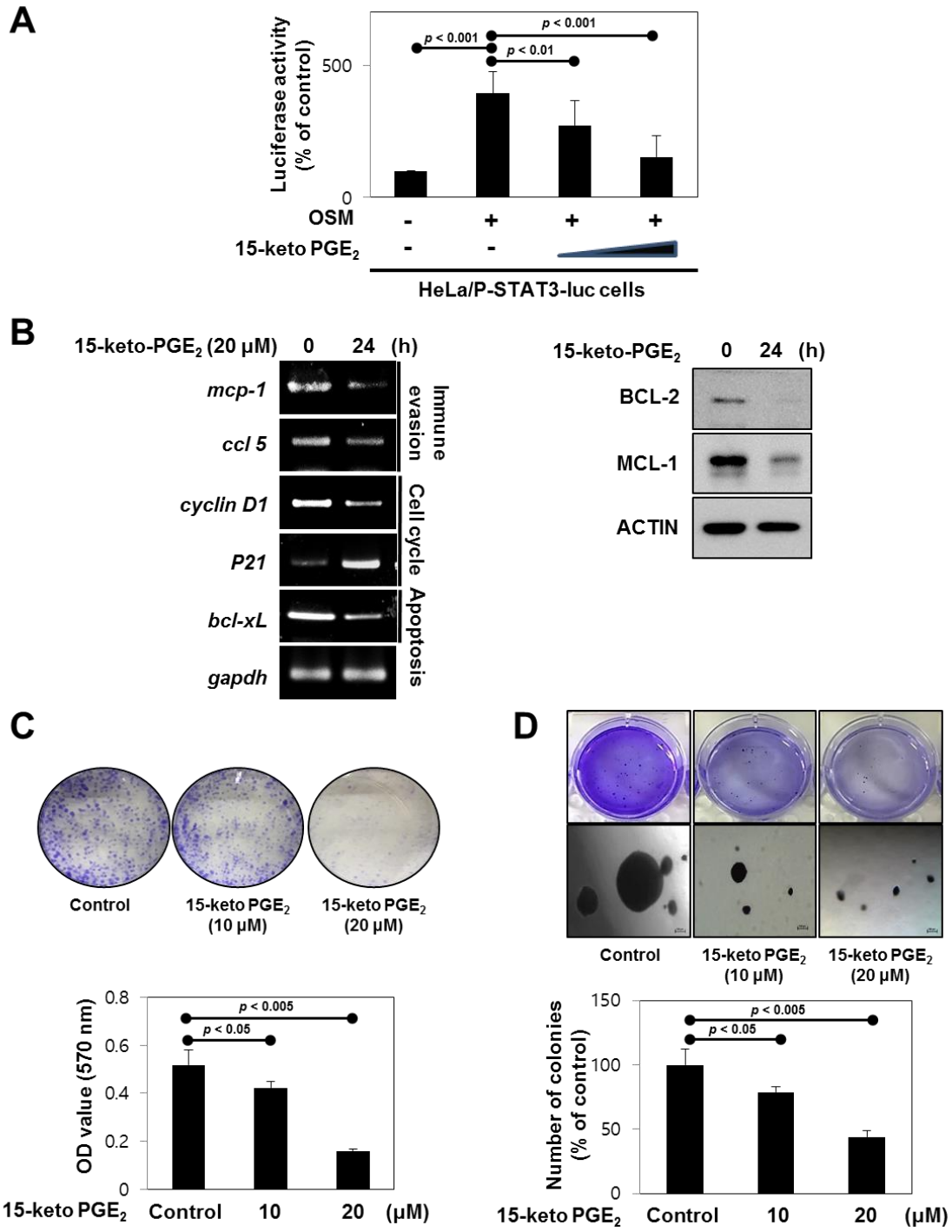

Figure 4. 15-Keto PGE_2-mediated inhibition of MCF10A-*ras* cell proliferation and growth through suppression of transcription of STAT3 target genes A. The luciferase assay was performed with HeLa/P-STAT3-Luc reporter cells. The cells were

treated with 15-keto PGE_2 (10 or 20 μM) for 24 h and then stimulated with Oncostatin M (10 ng/ml) for another 6 h. Cells were then analyzed by the microplate luminometer. **B.** The mRNA and protein levels of STAT3 target genes were determined by RT-PCR and Western blot analyses, respectively. MCF10A-*ras* cells were treated with 15-keto PGE_2 (20 μM) or vehicle for 24 h. GAPDH gene expression was measured to ensure equal amount of cDNA loaded. **C and D.** The clonogenic assay and the anchorage-independent growth assay were performed in MCF10A-*ras* cells. MCF10A-*ras* cells were seeded in 6 well plates and treated with two different concentrations of 15-keto PGE_2 (10 or 20 μM) or vehicle (DMSO) in 1 ml DMEM/F12 medium containing 5% heat-inactivated horse serum and supplementary agents. The soft agar colonies were counted under a light microscope. (colony size > 100 μm) For quantitative clonogenic assays, the colonies were solubilized with 10% acetic acid, and the absorbance at the wavelength of 540 nm was read. Results are the means ± S.D of triplicate experiments.

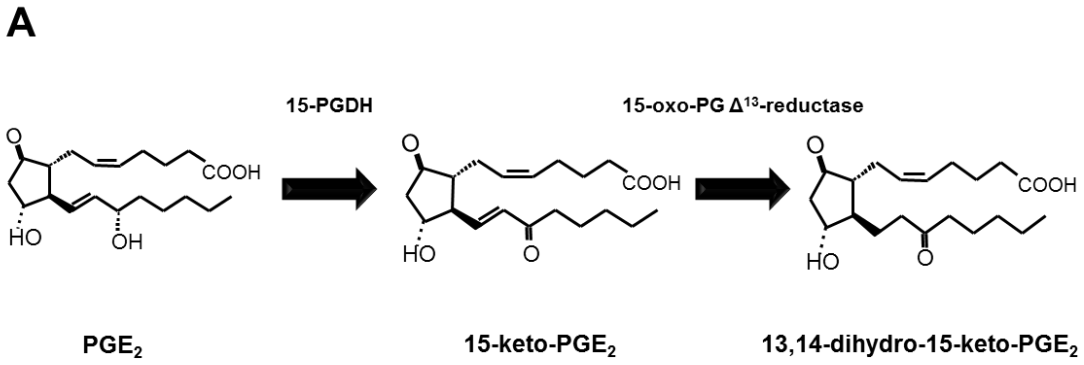
A
15-PGDH
15-oxo-PG Δ13-reductase
COOH
HO
OH
O
COOH
HO
O
COOH
HO
O
PGE2
15-keto-PGE2
13,14-dihydro-15-keto-PGE2

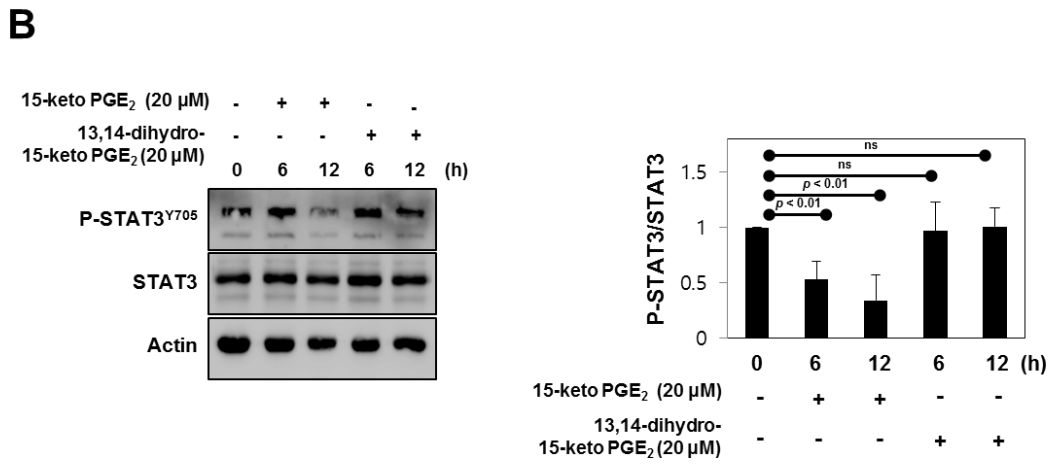
B
15-keto PGE2 (20 μM) - + + - -
13,14-dihydro-15-keto PGE2 (20 μM) - - - + +
0 6 12 6 12 (h)
P-STAT3Y705
STAT3
Actin
P-STAT3/STAT3
ns
ns
p < 0.01
p < 0.01
1.5
1
0.5
0
0 6 12 6 12 (h)
15-keto PGE2 (20 μM) - + + - -
13,14-dihydro-15-keto PGE2 (20 μM) - - - + +

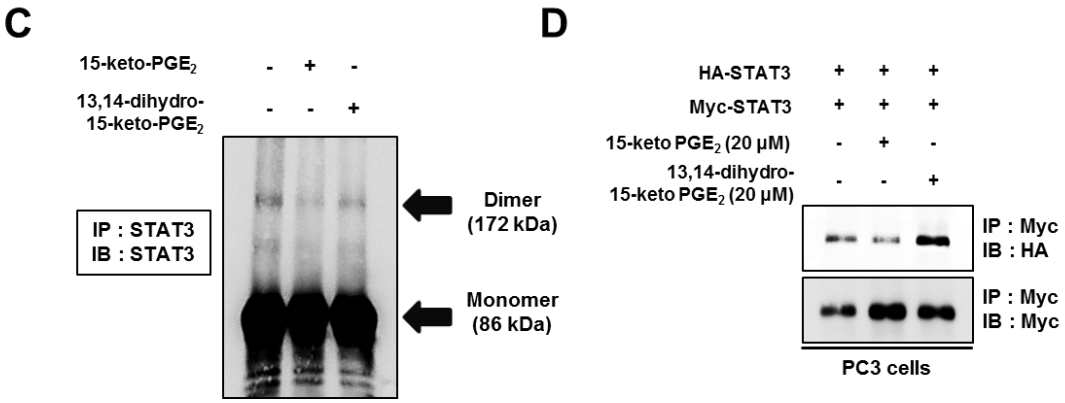
C
15-keto-PGE2 - + -
13,14-dihydro-15-keto-PGE2 - - +
IP : STAT3
IB : STAT3
Dimer
(172 kDa)
Monomer
(86 kDa)
D
HA-STAT3 + + +
Myc-STAT3 + + +
15-keto PGE2 (20 μM) - + -
13,14-dihydro-15-keto PGE2 (20 μM) - - +
IP : Myc
IB : HA
IP : Myc
IB : Myc
PC3 cells

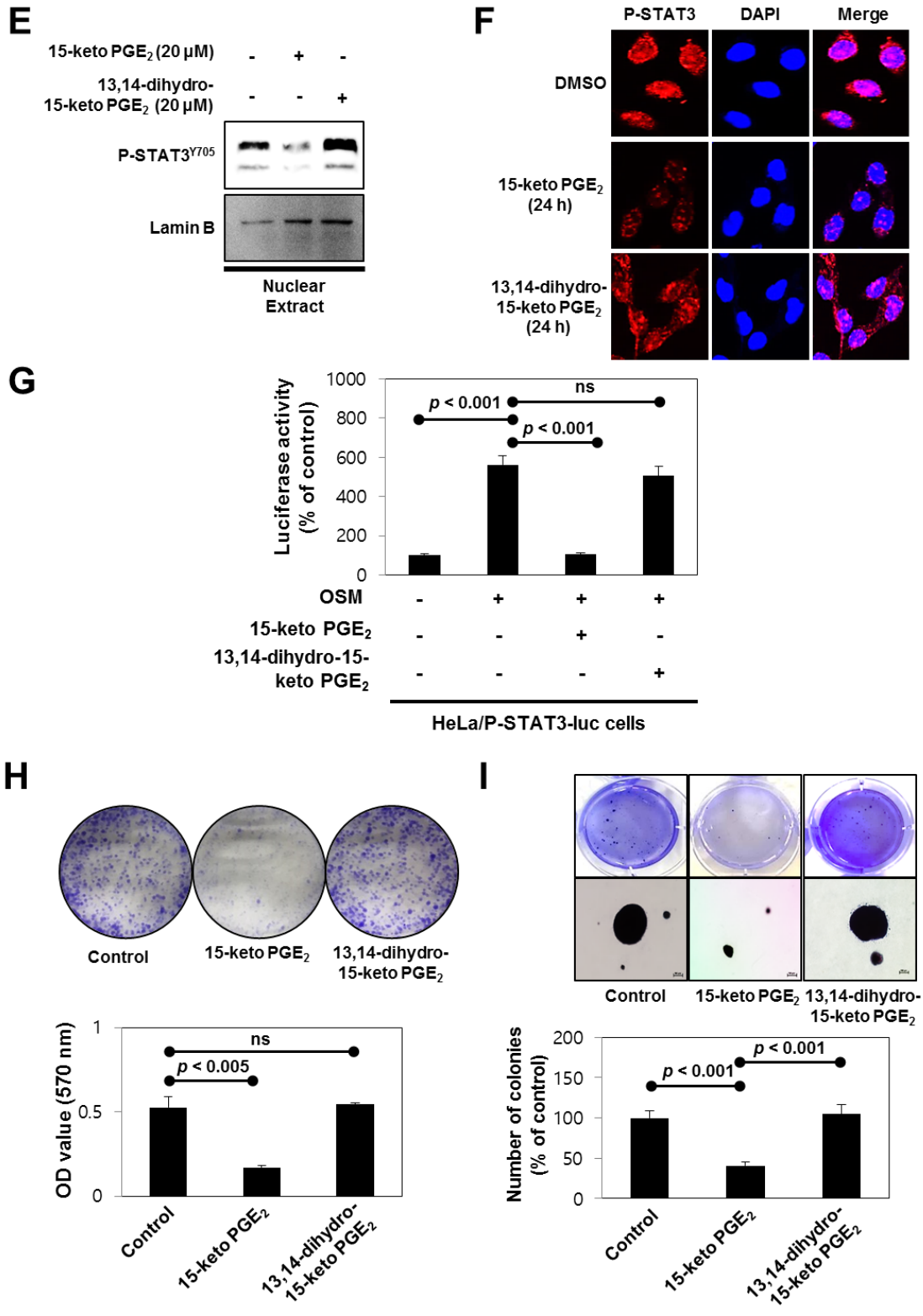

Figure 5. The involvement of the α,β-unsaturated carbonyl moiety of 15-Keto

PGE_2 in STAT3 deactivation A. 15-Keto PGE_2 has an α,β-unsaturated carbon which is considered to target nucleophiles whereas 13,14-dihydro-15-keto PGE_2, a metabolite of 15-keto PGE_2, has no such electrophilic moiety. **B.** MCF10A-*ras* cells were treated with 15-keto PGE_2 (20 μM) or 13,14-dihydro-15-keto PGE_2 (20 μM) for indicated time periods. The expression levels of P-STAT3^{Y705} and STAT3 were measured by Western blot analysis. **C.** Homodimerization of STAT3 was measured by the immunoprecipitation assay. MCF10A-*ras* cells were treated with 15-keto PGE_2 (20 μM) or 13,14-dihydro-15-keto PGE_2 (20 μM) for 12 h. **D.** Human prostate cancer PC3 cells were co-transfected with HA-tagged STAT3 and Myc-tagged STAT3 and treated with 15-keto PGE_2 or 13,14-dihydro-15-keto PGE_2 (20 μM each) for 12 h. The total lysates obtained from the transfected cells were immunoprecipitated with anti-Myc antibody and analyzed by Western blotting with anti-HA antibody. **E.** MCF10A-ras cells were incubated with 15-keto PGE_2 (20 μM) or 13,14-dihydro-15-keto PGE_2 (20 μM) for 24 h. The nuclear extracts were separated and subjected to Western blot analysis. **F.** After MCF10A-*ras* cells were treated with 15-keto PGE_2 (20 μM) or 13,14-dihydro-15-keto PGE_2 (20 μM) for 24 h, immunocytochemical analysis of P-STAT3^{Y705} was conducted. P-STAT3^{Y705} was detected using TRITC red fluorescence-labeled secondary antibody. **G.** The HeLa/P-STAT3-Luc reporter cells were pretreated with 15-keto PGE_2 (20 μM) or 13,14-dihydro-15-keto PGE_2 (20 μM) for 24 h followed by treatment with oncostatin M (OSM) for another 6 h. The cells were analyzed for the luciferase activity using a microplate luminometer. **H and I.** MCF10A-*ras* cells treated with 15-keto PGE_2 (20 μM) or 13,14-dihydro-15-keto PGE_2 (20 μM) were subjected to the clonogenic assay and the anchorage independent growth assay. The soft agar colonies were counted under a light microscope. (colony size > 100 μm) For quantitative clonogenic assays, the colonies

were solubilized with 10% acetic acid, and the absorbance at 540 nm was read. Results are the means ± S.D of triplicate experiments.

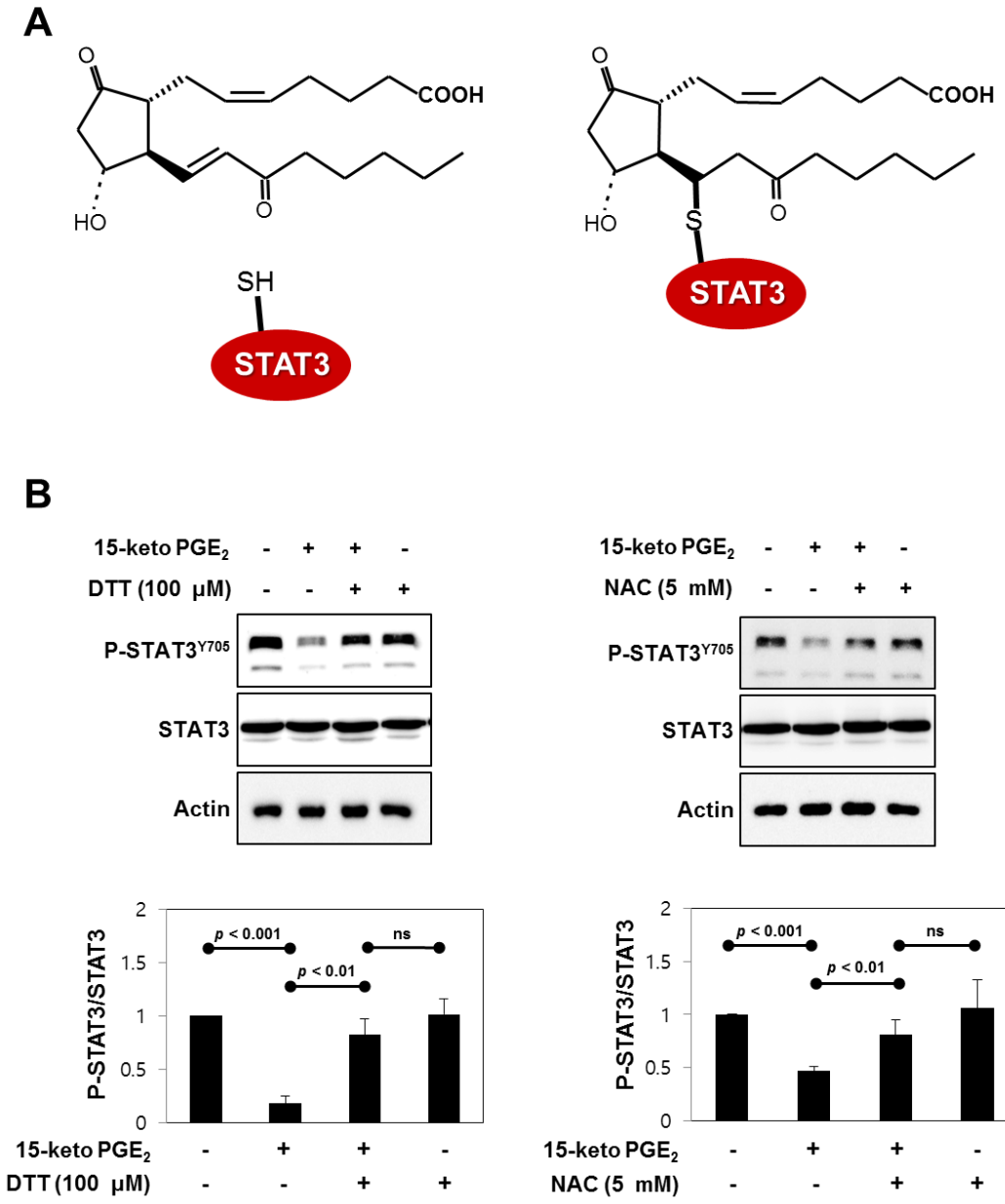
A
O
COOH
HO
O
SH
STAT3
O
COOH
HO
S
O
STAT3
B
15-keto PGE2 - + + -
DTT (100 μM) - - + +
P-STAT3Y705
STAT3
Actin
P-STAT3/STAT3
p < 0.001
p < 0.01
ns
15-keto PGE2 - + + -
DTT (100 μM) - - + +
15-keto PGE2 - + + -
NAC (5 mM) - - + +
P-STAT3Y705
STAT3
Actin
P-STAT3/STAT3
p < 0.001
p < 0.01
ns
15-keto PGE2 - + + -
NAC (5 mM) - - + +

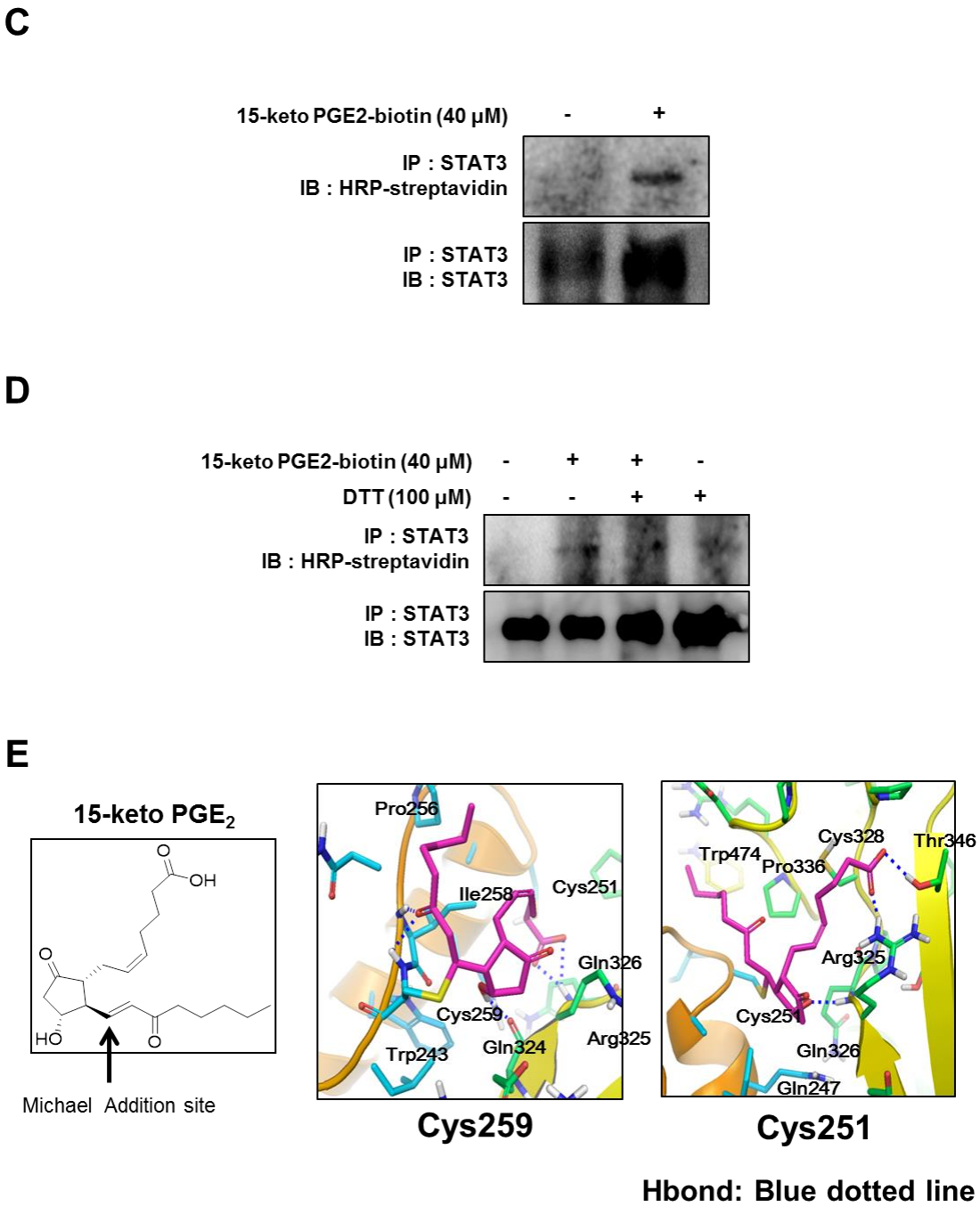

Figure 6. Covalent binding of 15-Keto PGE_2 to STAT3 via Michael addition reaction A. A proposed interaction between 15-keto PGE_2 and a thiol group of STAT3. **B.** MCF10A-*ras* cells were pretreated with thiol a reducing agent, DTT (100 μM) or NAC (5 mM), for 1 h followed by exposure to 15-keto PGE_2 (20 μM) for an additional

24 h. The protein levels of P-STAT3^{Y705} and STAT3 were determined by Western blot analysis. **C**. The direct binding of 15-keto PGE_2 to STAT3 was assessed using the biotin-streptavidin system. MCF10A-*ras* cells were exposed to biotinylated 15-keto PGE_2 (40 μM) for 24 h. The biotinylated 15-keto PGE_2-STAT3 complex was precipitated by monoclonal STAT3 antibody followed by immunoblot analysis with streptavidin-horse radish peroxidase secondary antibody. **D.** MCF10A-*ras* cells were pretreated with DTT (100 μM) or NAC (5 mM), for 1 h and then treated with biotinylated 15-keto PGE_2 (40 μM) for an additional 12 h. The biotinylated 15-keto PGE_2-STAT3 complex formation was determined by the immunoprecipitation and Western blot analyses. **E.** A putative model of 15-keto PGE_2 covalently binding to Cys^{259} and/or Cys^{251} of STAT3 as predicted by a docking study**.**

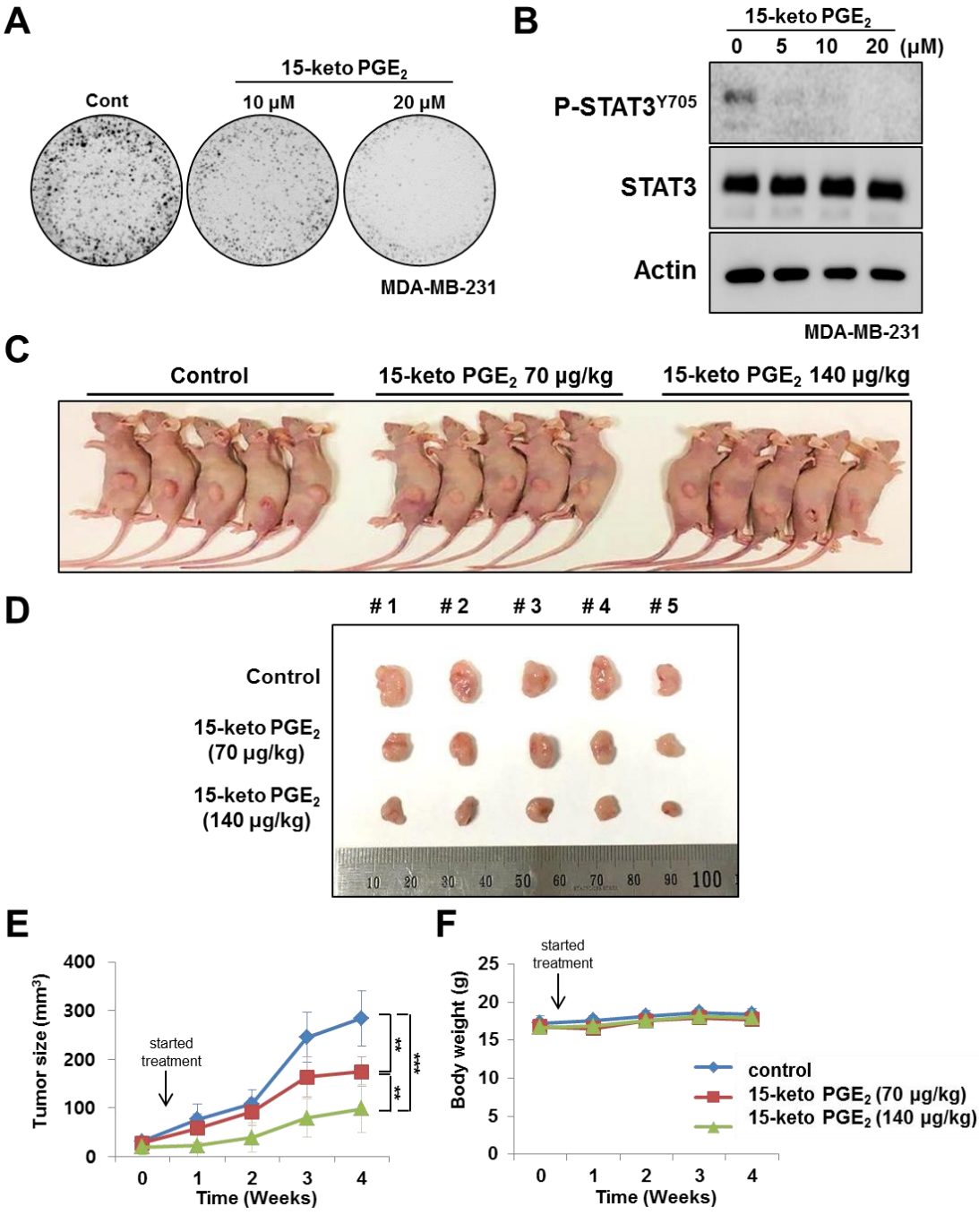
A
15-keto PGE2
Cont
10 μM
20 μM
MDA-MB-231
B
15-keto PGE2
0 5 10 20 (μM)
P-STAT3Y705
STAT3
Actin
MDA-MB-231
C
Control
15-keto PGE2 70 μg/kg
15-keto PGE2 140 μg/kg
D
1 # 2 # 3 # 4 # 5
Control
15-keto PGE2 (70 μg/kg)
15-keto PGE2 (140 μg/kg)
E
Tumor size (mm3)
started treatment
Time (Weeks)
F
Body weight (g)
started treatment
control
15-keto PGE2 (70 μg/kg)
15-keto PGE2 (140 μg/kg)
Time (Weeks)

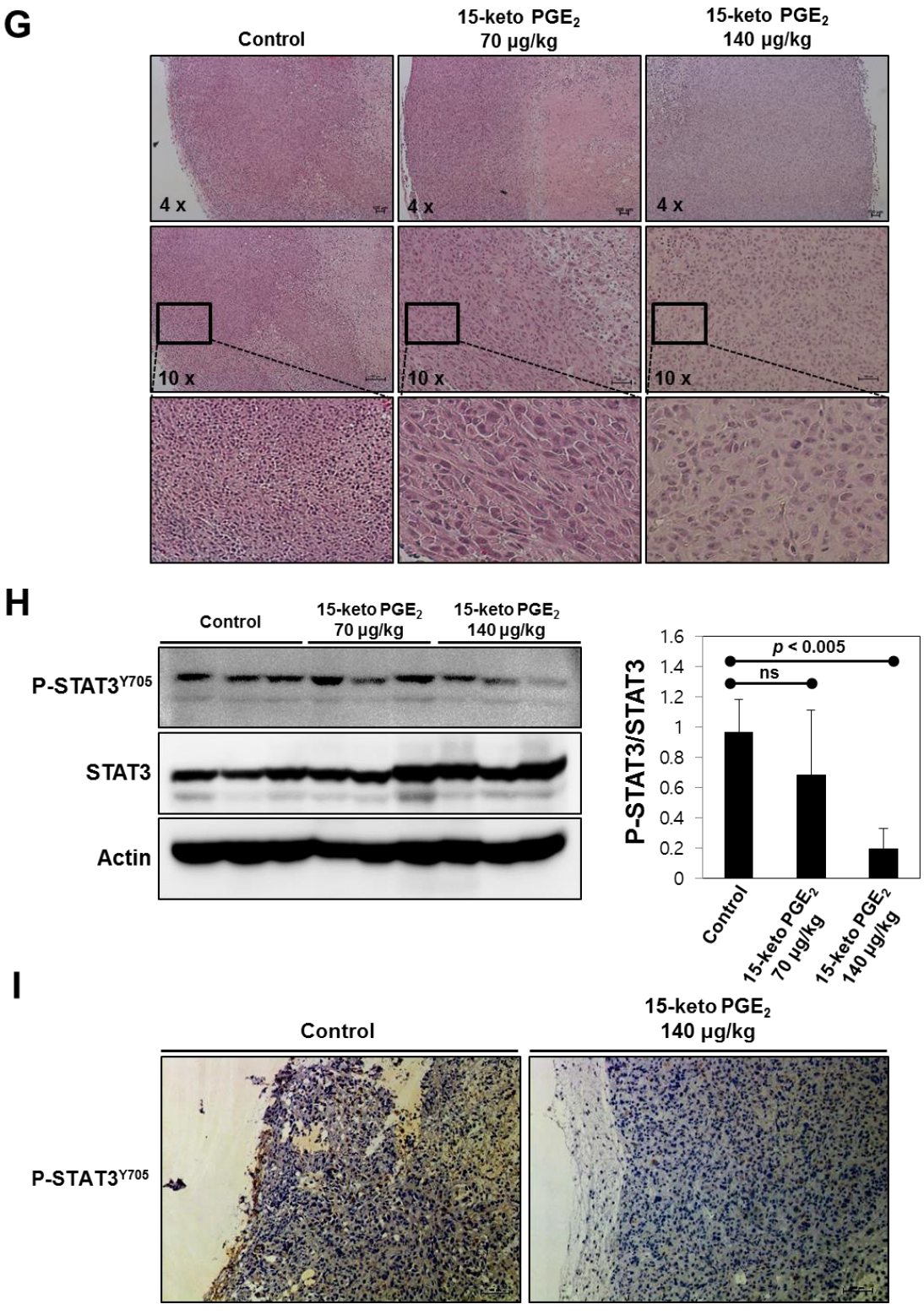

Figure 7. Suppression of tumor growth and STAT3 phosphorylation by 15-Keto

PGE_2 in a MDA-MB-231 xenograft model A. 15-keto PGE_2 (20 μM) treated MDA-MB-231 cells were subjected to the clonogenic assay. **B.** MDA-MB-231 cells were treated with 15-keto PGE_2 (20 μM) for 48 h. The expression levels of P-STAT3^{Y705} and STAT3 were measured by Western blot analysis. **C.** The representative shots of human mammary tumor (MDA-MB-231) xenografts in mice treated with vehicle, 15-keto PGE_2 (70 μg/kg) or 15-keto PGE_2 (140 μg/kg) for 4 weeks (n = 14/group). **D.** The size of tumors was measured with digital calipers. The calculated formula is 0.52 x length x width^2. ****** $p < 0.005$, ******* $p < 0.001$ (Two-sided t-test). **E**. The effect of 15-keto PGE_2 treatment on body weight. **G.** H&E stained tumor tissue sections. Scale bar : 100 μM. Magnification : x 4 and x 10. **H.** Total protein samples from the tumor specimens were subjected to measurement of the levels of P-STAT3^{Y705} and STAT3 by Western blot analysis. Actin was used as the internal control. **I.** The expression of P-STAT3^{Y705} was determined by immunohistochemical analysis in the tumor sections. Scale bar : 100 μM. Magnification : x 10

Discussion

PGE_2 is involved in chronic inflammation and it contributes to cancer development [3, 5]. PGE_2 and its receptors (EP1, EP2, EP3 and EP4) play important roles in promoting cancer progression [20-22, 33, 45]. PGE_2 exerts its function through EP receptors which are coupled to different signaling pathways [46-48]. STAT3 signaling was found to be inhibited by an EP receptor antagonist, which resulted in suppression of hepatocellular carcinoma cell growth [49]. As downstream effectors of PGE_2, activated EP receptors are involved in cancer progression. In mammary tumors, two subtypes of EP receptors, EP2 and EP4 are overexpressed. One study showed that mammary tumor angiogenesis and progression were suppressed through downregulation of EP2 and EP4 by a COX-2 inhibitor [47]. PGE_2 is rapidly metabolized to 15-keto PGE_2 [50]. A recent study suggests that 15-keto PGE_2 contributes to termination or attenuation of EP2 and EP4 responses [51]. Thus, 15-keto PGE_2 appears to exert anti-cancer effects through interruption of coupling PGE_2 and EP receptors. However, I found that 15-keto PGE_2 directly bound to STAT3. This suggests that the tumor suppressive effects of this lipid mediator may also arise from an EP receptor-independent mechanism.

Numerous human cancers harbor persistently activated STAT3 which induces tumor formation, growth and survival [13, 16]. Accumulating evidence indicates that PGE_2 has a close association with the STAT3 signaling pathway [20-22, 49]. JAK2 is one of STAT3 upstream kinases, and the JAK2/STAT3 pathway has been extensively investigated in breast and other cancer types [52]. Inhibition of JAK2 activity deactivates STAT3 in most breast cancer cells [53]. Given the importance of the JAK2/STAT3 axis in cancer, inhibiting this kinase seems to be a reasonable approach.

However, a recent study suggested that a JAK2 inhibitor, cucurbitacin I, also affected the actin cytoskeleton in non-tumor cells [54]. Furthermore, some studies demonstrated that JAK2 inhibits tumor initiation as a tumor suppresser [55-57]. Therefore, direct inhibition of STAT3 could be more effective strategy to inhibit cancer progression. Interestingly, I observed that 15-keto PGE_2 selectively inhibited STAT3 phosphorylation without affecting the JAK2 activity or the SOCS3 expression.

PPARγ is a member of nuclear receptor superfamily, which functions as ligand-dependent activators of transcription [58]. PPARγ ligands have been shown to inhibit cell growth and induce apoptosis in several types of human cancer, suggesting that this transcription factor may be a tumor suppressor gene [36]. One study showed that an endogenous PPARγ ligand, 15-deoxy-$\Delta^{12,14}$-prostaglandin J_2 (15d-PGJ_2) effectively blocked DNA binding and transcriptional activity of STAT3 through activation of PPARγ [59]. I attempted to investigate whether the inhibitory effect of 15-keto PGE_2 on STAT3 activation is mediated by PPARγ. 15-Keto PGE_2 inhibits STAT3 signaling in MCF10A-*ras* cells, which was unlikely to be dependent on PPARγ activation. This suggests that there may be an alternative mechanism for blocking STAT3 signaling by 15-keto PGE_2. 15-Keto PGE_2 has an electrophilic α,β-unsaturated carbonyl group that can covalently modify nucleophilic cysteine residue(s) present in various proteins, regulating their functions/activities [30, 60, 61]. In the present study, 15-keto PGE_2 formed an adduct with thiol group(s) of cysteine residue(s) in STAT3. STAT3 signaling was inhibited by 15-keto PGE_2 but not by 13,14-dihydro-15-keto PGE_2 which lacks the α,β-unsaturated carbonyl group. The direct interaction between 15-keto PGE_2 and STAT3 was disrupted by thiol reducing agents, such as DTT or NAC. Above results suggest that the Michael addition reaction occurs between the α,β-unsaturated carbonyl

group of 15-keto PGE_2 and cysteine residue(s) in STAT3.

STAT3 consists of 6 domains. These include N-terminal domain (ND), a coiled-coil domain (CCD), a DNA binding domain (DBD), a linker domain (LK), Src-homology 2 (SH2) domain and C-terminal transactivation domain. Recent studies suggest that alkylation of a cysteine residue in STAT3 is a plausible mechanism of STAT3 inhibition [62, 63]. A small molecule compound, NSC-368262 (C48) alkylates Cys^{468} in DNA binding domain of STAT3, thereby suppressing DNA binding of this transcription factor [64]. A docking study predicted Cys^{251} and Cys^{259} in STAT3 as preferential targets for a covalent linkage formation with 15-keto PGE_2. These two cysteine residues are located in the coiled-coil domain of STAT3. It is well known that the SH2 domain of STAT3 is essential for binding to an activated receptor, gp130 and that STAT3 is phosphorylated by the gp130-associated JAKs [65, 66]. However, one study demonstrated that the coiled-coil domain also interacts directly with the gp130 peptide and is required for STAT3 phosphorylation [66]. It is therefore plausible that 15-keto PGE_2 inhibits STAT3 phosphorylation by binding to this domain. It still remains to be investigated which cysteine residue(s) is/are likely to be the site(s) for 15-keto PGE_2 to target.

The tumor suppressive potential of 15-keto PGE_2 was evaluated in human mammary tumor xenograft model. The growth of MDA-MB-231 xenograft tumors was suppressed by subcutaneous treatment of 15-keto PGE_2 without significant side effects. Furthermore, STAT3 phosphorylation was significantly inhibited in the high dose-treated group. In conclusion, 15-keto PGE_2 inhibits STAT3 signaling by covalently modifying this protein, thereby suppressing breast cancer proliferation and growth.

References

1. Nakanishi, M. and D.W. Rosenberg, Multifaceted roles of PGE2 in inflammation and cancer. Semin Immunopathol 2013;**35**(2):123-37.
2. Rigas, B., I.S. Goldman, and L. Levine, Altered eicosanoid levels in human colon cancer. J Lab Clin Med 1993;**122**(5):518-23.
3. Wang, D. and R.N. Dubois, Eicosanoids and cancer. Nat Rev Cancer 2010;**10**(3):181-93.
4. Schrey, M.P. and K.V. Patel, Prostaglandin E2 production and metabolism in human breast cancer cells and breast fibroblasts. Regulation by inflammatory mediators. Br J Cancer 1995;**72**(6):1412-9.
5. Howe, L.R., Inflammation and breast cancer. Cyclooxygenase/prostaglandin signaling and breast cancer. Breast Cancer Res 2007;**9**(4):210.
6. Marnett, L.J. and R.N. DuBois, COX-2: a target for colon cancer prevention. Annu Rev Pharmacol Toxicol 2002;**42**:55-80.
7. Hull, M.A., S.C. Ko, and G. Hawcroft, Prostaglandin EP receptors: targets for treatment and prevention of colorectal cancer? Mol Cancer Ther 2004;**3**(8):1031-9.
8. Reader, J., D. Holt, and A. Fulton, Prostaglandin E2 EP receptors as therapeutic targets in breast cancer. Cancer Metastasis Rev 2011;**30**(3-4):449-63.
9. Greenhough, A., et al., The COX-2/PGE2 pathway: key roles in the hallmarks of cancer and adaptation to the tumour microenvironment. Carcinogenesis 2009;**30**(3):377-86.
10. Legler, D.F., et al., Prostaglandin E2 at new glance: novel insights in functional diversity offer therapeutic chances. Int J Biochem Cell Biol 2010;**42**(2):198-201.
11. Wang, M.T., K.V. Honn, and D. Nie, Cyclooxygenases, prostanoids, and tumor progression. Cancer Metastasis Rev 2007;**26**(3-4):525-34.
12. Levy, D.E. and J.E. Darnell, Jr., Stats: transcriptional control and biological impact. Nat Rev Mol Cell Biol 2002;**3**(9):651-62.
13. Turkson, J., STAT proteins as novel targets for cancer drug discovery. Expert Opin Ther Targets 2004;**8**(5):409-22.
14. Darnell, J.E., Jr., STATs and gene regulation. Science 1997;**277**(5332):1630-5.
15. Aggarwal, B.B., et al., Signal transducer and activator of transcription-3, inflammation, and cancer: how intimate is the relationship? Ann N Y Acad Sci 2009;**1171**:59-76.
16. Yue, P. and J. Turkson, Targeting STAT3 in cancer: how successful are we? Expert Opin Investig Drugs 2009;**18**(1):45-56.

17. Banerjee, K. and H. Resat, Constitutive activation of STAT3 in breast cancer cells: A review. Int J Cancer 2016;**138**(11):2570-8.
18. Inghirami, G., et al., New and old functions of STAT3: a pivotal target for individualized treatment of cancer. Cell Cycle 2005;**4**(9):1131-3.
19. Liu, D.B., et al., Celecoxib induces apoptosis and cell-cycle arrest in nasopharyngeal carcinoma cell lines via inhibition of STAT3 phosphorylation. Acta Pharmacol Sin 2012; **33**(5):682-90.
20. Dalwadi, H., et al., Cyclooxygenase-2-dependent activation of signal transducer and activator of transcription 3 by interleukin-6 in non-small cell lung cancer. Clin Cancer Res 2005;**11**(21):7674-82.
21. Liu, Q., et al., Metformin represses bladder cancer progression by inhibiting stem cell repopulation via COX2/PGE2/STAT3 axis. Oncotarget 2016;**7**(19):28235-46.
22. Liu, X., et al., Berberine Inhibits Invasion and Metastasis of Colorectal Cancer Cells via COX-2/PGE2 Mediated JAK2/STAT3 Signaling Pathway. PLoS One 2015;**10**(5): e0123478.
23. Tai, H.H., Prostaglandin catabolic enzymes as tumor suppressors. Cancer Metastasis Rev 2011;**30**(3-4):409-17.
24. Chang, E.Y., et al., Inhibition of Prostaglandin Reductase 2, a Putative Oncogene Overexpressed in Human Pancreatic Adenocarcinoma, Induces Oxidative Stress-Mediated Cell Death Involving xCT and CTH Gene Expressions through 15-Keto-PGE2. PLoS One 2016;**11**(1):e0147390.
25. Lu, D., C. Han, and T. Wu, 15-PGDH inhibits hepatocellular carcinoma growth through 15-keto-PGE2/PPARgamma-mediated activation of p21WAF1/Cip1. Oncogene 2014;**33**(9):1101-12.
26. Chou, W.L., et al., Identification of a novel prostaglandin reductase reveals the involvement of prostaglandin E2 catabolism in regulation of peroxisome proliferator-activated receptor gamma activation. J Biol Chem 2007;**282**(25):18162-72.
27. Shibata, T., 15-Deoxy-Delta(1)(2),(1)(4)-prostaglandin J(2) as an electrophilic mediator. Biosci Biotechnol Biochem 2015;**79**(7):1044-9.
28. Cernuda-Morollon, E., et al., 15-Deoxy-Delta 12,14-prostaglandin J2 inhibition of NF-kappaB-DNA binding through covalent modification of the p50 subunit. J Biol Chem 2001;**276**(38):35530-6.
29. Perez-Sala, D., E. Cernuda-Morollon, and F.J. Canada, Molecular basis for the direct inhibition of AP-1 DNA binding by 15-deoxy-Delta 12,14-prostaglandin J2. J Biol Chem 2003;**278**(51):51251-60.

30. Shiraki, T., et al., Alpha,beta-unsaturated ketone is a core moiety of natural ligands for covalent binding to peroxisome proliferator-activated receptor gamma. J Biol Chem 2005; **280**(14):14145-53.
31. Sato, Y., et al., The AMeX method. A simplified technique of tissue processing and paraffin embedding with improved preservation of antigens for immunostaining. Am J Pathol 1986;**125**(3):431-5.
32. Na, H.K., et al., 15-Hydroxyprostaglandin dehydrogenase as a novel molecular target for cancer chemoprevention and therapy. Biochem Pharmacol, 2011. **82**(10): p. 1352-60.
33. Liu, X.H., et al., Prostaglandin E(2) stimulates prostatic intraepithelial neoplasia cell growth through activation of the interleukin-6/GP130/STAT-3 signaling pathway. Biochem Biophys Res Commun 2002;**290**(1):249-55.
34. Watson, J. and S.Y. Chuah, Technique for the primary culture of human breast cancer cells and measurement of their prostaglandin secretion. Clin Sci (Lond) 1992;**83**(3): 347-52.
35. Yu, H., et al., Revisiting STAT3 signalling in cancer: new and unexpected biological functions. Nat Rev Cancer 2014;**14**(11):736-46.
36. Koeffler, H.P., Peroxisome proliferator-activated receptor gamma and cancers. Clin Cancer Res 2003; **9**(1):1-9.
37. Berishaj, M., et al., Stat3 is tyrosine-phosphorylated through the interleukin-6/glycoprotein 130/Janus kinase pathway in breast cancer. Breast Cancer Res 2007; **9**(3):R32.
38. Sansone, P. and J. Bromberg, Targeting the interleukin-6/Jak/stat pathway in human malignancies. J Clin Oncol 2012;**30**(9):1005-14.
39. Carow, B. and M.E. Rottenberg, SOCS3, a Major Regulator of Infection and Inflammation. Front Immunol 2014; **5**:58.
40. Furtek, S.L., et al., Strategies and Approaches of Targeting STAT3 for Cancer Treatment. ACS Chem Biol 2016;**11**(2):308-18.
41. Carpenter, R.L. and H.W. Lo, STAT3 Target Genes Relevant to Human Cancers. Cancers (Basel) 2014;**6**(2): 897-925.
42. Dauer, D.J., et al., Stat3 regulates genes common to both wound healing and cancer. Oncogene 2005;**24**(21):3397-408.
43. Cipollina, C., Endogenous Generation and Signaling Actions of Omega-3 Fatty Acid Electrophilic Derivatives. Biomed Res Int 2015;**2015**:501792.
44. Yu, X., et al., Eriocalyxin B Inhibits STAT3 Signaling by Covalently Targeting STAT3 and Blocking Phosphorylation and Activation of STAT3. PLoS One

2015;**10**(5):e0128406.

45. Wang, D. and R.N. Dubois, Prostaglandins and cancer. Gut 2006;**55**(1):115-22.
46. Castellone, M.D., et al., Prostaglandin E2 promotes colon cancer cell growth through a Gs-axin-beta-catenin signaling axis. Science 2005;**310**(5753):1504-10.
47. Chang, S.H., et al., Role of prostaglandin E2-dependent angiogenic switch in cyclooxygenase 2-induced breast cancer progression. Proc Natl Acad Sci U S A 2004;**101**(2):591-6.
48. Chell, S.D., et al., Increased EP4 receptor expression in colorectal cancer progression promotes cell growth and anchorage independence. Cancer Res 2006;**66**(6): 3106-13.
49. Lin, A., et al., TLR4 signaling promotes a COX-2/PGE2/STAT3 positive feedback loop in hepatocellular carcinoma (HCC) cells. Oncoimmunology 2016;**5**(2):e1074376.
50. Tai, H.H., et al., Prostaglandin catabolizing enzymes. Prostaglandins Other Lipid Mediat 2002; **68-69**:483-93.
51. Nishigaki, N., M. Negishi, and A. Ichikawa, Two Gs-coupled prostaglandin E receptor subtypes, EP2 and EP4, differ in desensitization and sensitivity to the metabolic inactivation of the agonist. Mol Pharmacol 1996;**50**(4):1031-7.
52. Bollrath, J. and F.R. Greten, IKK/NF-kappaB and STAT3 pathways: central signalling hubs in inflammation-mediated tumour promotion and metastasis. EMBO Rep 2009;**10**(12):1314-9.
53. Marotta, L.L., et al., The JAK2/STAT3 signaling pathway is required for growth of CD44(+)CD24(-) stem cell-like breast cancer cells in human tumors. J Clin Invest 2011;**121**(7):2723-35.
54. Graness, A., V. Poli, and M. Goppelt-Struebe, STAT3-independent inhibition of lysophosphatidic acid-mediated upregulation of connective tissue growth factor (CTGF) by cucurbitacin I. Biochem Pharmacol 2006;**72**(1):32-41.
55. Chawla-Sarkar, M., et al., Apoptosis and interferons: role of interferon-stimulated genes as mediators of apoptosis. Apoptosis 2003;**8**(3):237-49.
56. Gresser, I., Antitumor effects of interferon. Adv Cancer Res 1972;**16**:97-140.
57. Vindrieux, D., et al., PLA2R1 mediates tumor suppression by activating JAK2. Cancer Res 2013;**73**(20):6334-45.
58. Debril, M.B., et al., The pleiotropic functions of peroxisome proliferator-activated receptor gamma. J Mol Med (Berl) 2001;**79**(1):30-47.
59. Wang, L.H., et al., Transcriptional inactivation of STAT3 by PPARgamma suppresses IL-6-responsive multiple myeloma cells. Immunity 2004;**20**(2):205-18.
60. Oh, J.Y., et al., Accumulation of 15-deoxy-delta(12,14)-prostaglandin J2 adduct

formation with Keap1 over time: effects on potency for intracellular antioxidant defence induction. Biochem J 2008;**411**(2):297-306.

61. Sanchez-Gomez, F.J., et al., Protein thiol modification by 15-deoxy-Delta12,14-prostaglandin J2 addition in mesangial cells: role in the inhibition of pro-inflammatory genes. Mol Pharmacol 2004;**66**(5):1349-58.
62. Ahmad, R., et al., Triterpenoid CDDO-methyl ester inhibits the Janus-activated kinase-1 (JAK1)-->signal transducer and activator of transcription-3 (STAT3) pathway by direct inhibition of JAK1 and STAT3. Cancer Res 2008;**68**(8):2920-6.
63. Don-Doncow, N., et al., Galiellalactone is a direct inhibitor of the transcription factor STAT3 in prostate cancer cells. J Biol Chem 2014;**289**(23):15969-78.
64. Buettner, R., et al., Alkylation of cysteine 468 in Stat3 defines a novel site for therapeutic development. ACS Chem Biol 2011;**6**(5):432-43.
65. Stahl, N., et al., Choice of STATs and other substrates specified by modular tyrosine-based motifs in cytokine receptors. Science 1995;**267**(5202):1349-53.
66. Zhang, T., et al., The coiled-coil domain of Stat3 is essential for its SH2 domain-mediated receptor binding and subsequent activation induced by epidermal growth factor and interleukin-6. Mol Cell Biol 2000;**20**(19):7132-9.

국문초록

Prostaglandin E_2 (PGE_2)는 염증반응과 암화과정에서 대량으로 생성된다. 과발현한 PGE_2 는 암세포의 증식과 암세포사멸 저항성, 암세포 전이와 관련이 있다. PGE_2 는 15-hydroxyprostaglandin dehydrogenase (15-PGDH)에 의해 산화되어 15-keto prostaglandin E_2 (15-keto PGE_2)로 전환된다. 15-keto PGE_2 는 이제까지 PGE_2 의 생리불활성 형태로서 알려져 있다. 그러나, 최근 연구에 따르면 15-keto PGE_2 는 여러 종양활성신호를 차단함으로써 종양 억제 효과가 있음을 입증되었다. 그러나 이에 따른 분자적 기전연구에 대해서는 연구가 많이 되어있지 않다.

Signal transducer and activator of transcription factor 3 (STAT3)는 전사인자로 세포 증식을 유도하면서 동시에 세포 사멸 저항성을 가지고 있다. 정상세포와는 다르게 많은 암세포에서 STAT3 는 활성화 상태를 계속 유지하고 있다. 지속적으로 활성화된 STAT3 는 발암과 암화과정에서 주요한 역할을 한다. 이러한 STAT3 신호전달과정이 15-PGDH 에 의하여 억제된다는 보고가 있지만 그에 따른 분자적 기전연구에 대해서는 이루어지지 않았다. 따라서 본 연구에서는 15-PGDH 에 의해 생성된 대사물질인 15-keto PGE_2 가 STAT3 불활성화 효과가 있는지 확인하였다.

또한, 암유전자 Ha-*Ras* 가 도입된 인체유방세포 (MCF10A-*ras*)에서 15-keto PGE_2 의 구조적 특징인 α,β 불포화 카보닐기가 STAT3 신호전달과정인 인산화와 이량체 형성, 핵내 이동 억제효과에 주요한 역할을 한다는 것을 밝혔다. α,β 불포화 카보닐기는 친전자성을 가지고 있지만 그에 비해 α,β 불포화 카보닐기가 없는 13,14-dihydro-15-keto Prostaglandin E_2 (13,14-dihydro-15-keto PGE_2)는 친전자성을 가지고 있지 않다. Ha-*Ras* 가 도입된 인체유방세포 (MCF10A-*ras*)에서 13,14-dihydro-15-keto PGE_2 는 15-keto PGE_2 와 다른 양상으로, STAT3 신호전달 억제효과가 없었고, 그에 따라서 암세포 증식억제 효과 역시 미비하였다.

이러한 친전자성을 띄는 15-keto PGE_2 의 α,β 불포화 카보닐기가 STAT3 시스틴 잔기의 티올기와 결합하여 STAT3 활성 억제 가능성을 확인하였다. 15-keto PGE_2 는 STAT3 와 직접적인 결합을 하고, 그에 따라 STAT3 불활성을 유도함을 확인하였지만, 티올기 환원제로 알려져 있는 dithiothreitol (DTT) 또는 N-acetyl-L-cysteine (NAC)을 처리하였을 때 15-keto PGE_2 에 의한 STAT3 불활성화와 서로 간의 직접적인 결합은

이루어지지 않았다. Computer docking modeling 에서 15-keto PGE_2 가 STAT3 시스틴 잔기 251 번과 259 번에 직접 결합 가능성을 제시하였다.

다른 인체 유방암세포인 MDA-MB-231 에서 역시 15-keto PGE_2 에 의해 STAT3 가 불활성화 되었고, 암세포 증식이 억제되었다. MDA-MB-231 세포를 주입한 누드마우스 모델에서 역시 15-keto PGE_2 에 의해 종양생성이 약화되었고, 활성화된 STAT3 발현 역시 감소되었음을 확인하였다. 본 연구에 따르면 15-keto PGE_2 가 STAT3 와의 직접적인 결합과정에서 시스틴 잔기의 티올기를 변형하여 불활성화를 유도하고, 그에 따라 인체 유방암세포의 증식과 성장이 억제됨을 규명하였다.

주요어: 15-Keto PGE2, 친전자성, α,β 불포화 카보닐기, STAT3, 티올기 변화, MCF10A-ras, MDA-MB-231 동물 모델

학 번: 2015-26014